

## MAXIMIZATION OF TUNGSTEN CRYSTALLITES FROM DIRECTLY REDUCED AMMONIUM PARATUNGSTATE

JAMES G. LAKE\* AND W. RICHARD OTT

*Department of Ceramics, College of Engineering, Rutgers, The State University, New Brunswick, New Jersey (U.S.A.)*

(Received 9 October 1978)

### ABSTRACT

The reduction of tungsten directly from ammonium paratungstate has been studied to maximize the crystallite size. The decomposition and reduction sequences were monitored by thermal analysis and analyzed by X-ray diffraction and scanning electron microscopy. The tungsten crystallite size was seen to increase with faster heating rates, larger samples sizes, slower hydrogen flows over the sample and with a sealed reaction vessel. This appears to be the result of retarding the nucleation of tungsten nuclei by controlling the rate at which reaction products are removed from the reaction site. Consequently a smaller number of nuclei grow to larger sizes.

The ammonium paratungstate powder was characterized by composition, morphology and bulk density.

### INTRODUCTION

Following World War I, revolutionary changes in the metal working industry came about because of rapid advances in cemented carbide materials. These materials permitted improved efficiency in the high speed machining of steel. Tungsten carbide-cobalt composites were the first of these materials to gain widespread commercial importance. An appealing blend of properties was derived from these composites. The carbide phase contributes great hardness and the metal binder contributes toughness and strength to a sinterable compact.

A mixture of metallic tungsten and carbon black are normally reacted to form the desired carbide phase. The tungsten metal comes from the reduction of various raw material sources. Tungsten trioxide, tungstic acid and ammonium paratungstate are the major raw materials used in the manufacture of tungsten metal which is developed into tungsten carbide. However, the least expensive raw material is ammonium paratungstate when it is reduced in a single step to tungsten metal. Attempts

---

\* Present address: V. R. Wesson Inc., Chicago, Illinois, U.S.A. This research is based on work submitted by Dr. Lake in partial fulfillment of the requirements for the Ph.D. degree.

to use ammonium paratungstate in industrial applications have not been successful because the resulting crystallite size has been too small to meet the requirements for existing grades of tungsten carbide.

Microstructure plays an important role in the mechanical properties of cobalt bonded tungsten carbide. Starting with the tungsten metal powder, careful control over the tungsten crystallite size is important. It has been demonstrated, that the crystallite size of the tungsten metal has a direct bearing on the grain size of the carburized tungsten carbide. The carburizing conditions have also been shown to influence the grain size of the resultant tungsten carbide, but the crystallite size of the tungsten metal has been shown by Hara and Miyake<sup>1-3</sup> and Miyoshi and Doi<sup>4</sup> to be the ultimate limiting factor in the maximization of the size of the tungsten carbide grain.

Processes taking place during the sintering of the cobalt bonded tungsten carbide have been shown to cause additional changes in the grain size of the sintered material. Grain growth and even exaggerated grain growth occur due to the nature of liquid phase sintering, whereby, small grains are taken into solution and then are reprecipitated onto the surface of the larger grains. This effect can be minimized by use of grain growth inhibitors or by the size and nature of the carburized tungsten. Thus, the size of the tungsten has been shown to influence the size of the sintered tungsten carbide grain; directly, in the case where no grain growth results or indirectly, where grain growth occurs. This study has attempted to maximize the tungsten crystallite size and also to gain an understanding of the effects of time, temperature and atmosphere on the resultant crystallite size.

#### LITERATURE REVIEW

The mechanical properties of cobalt bonded tungsten carbide are a compromise between the competing requirements for hardness and for toughness. The tungsten carbide phase is hard and brittle, while the cobalt binder is relatively soft and ductile, together they are combined into a cemented carbide which is hard and strong.

The hardness of cobalt bonded tungsten carbide is mainly contributed by the carbide phase and toughness or strength by the cobalt phase. Manufacturers of these materials adjust the cobalt content, the carbide grain size and the carbon chemistry to obtain the desired combination of hardness and strength for specific grades of material. Commercial grades of cobalt cemented tungsten carbide have cobalt contents between 5 and 25 wt.%. Yield stress and hardness decrease with increasing cobalt content, but tensile strength reaches a maximum value at intermediate compositions<sup>5</sup>.

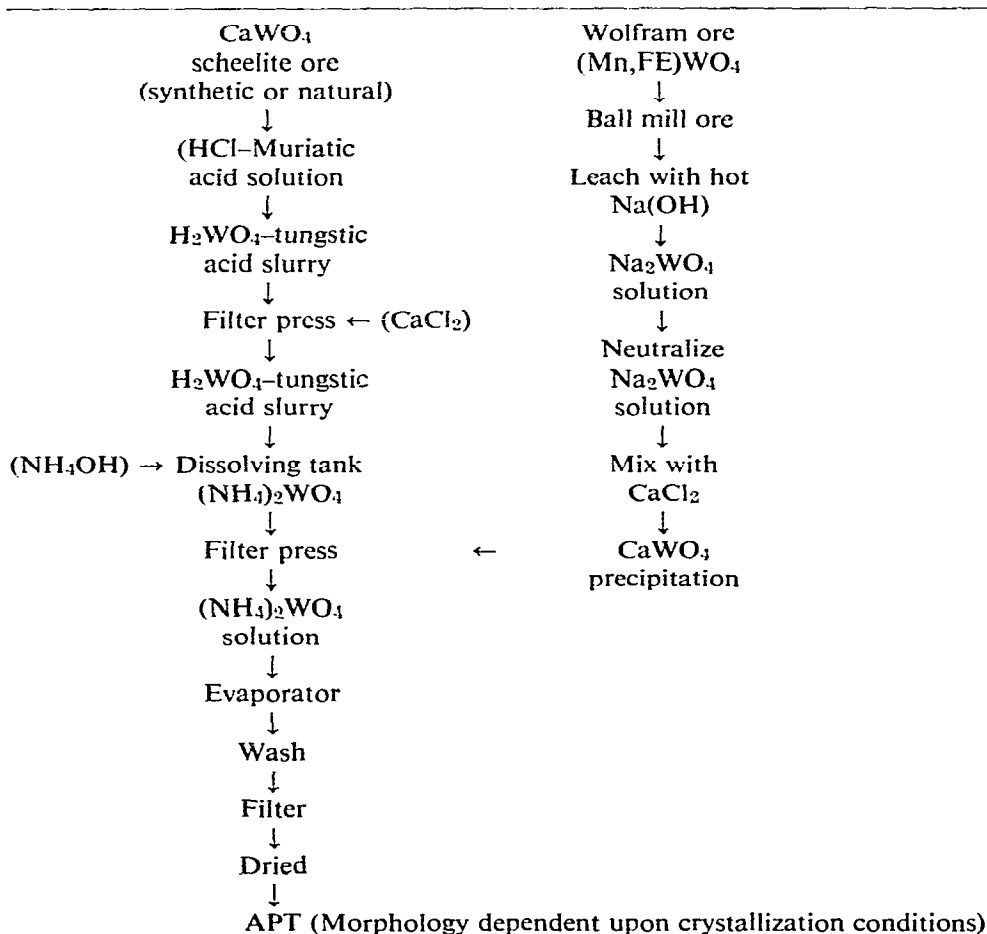
Hardness of cemented carbides is affected by microporosity, but is most strongly influenced by the carbide grain size and by the composition of the carbide phase<sup>6-8</sup>. The degree of dispersion of the cobalt and the carbide phases also may influence hardness. The hardness has been found to decrease as the particle size increases (from 1 to 6  $\mu\text{m}$ ) for a fixed cobalt content<sup>9-11</sup>.

Gurland and Bardzil<sup>12</sup> and Norton<sup>13</sup> studied the influence of grain size on the transverse-rupture strength of cobalt-tungsten carbide composites. Their studies concluded that the modulus of rupture exhibits a maximum at an average carbide grain size between 3 and 4  $\mu\text{m}$  in diameter for a composite of 88 wt. % WC and 12 wt. % Co. These results were confirmed by Ingelstrom and Nordberg<sup>14</sup> over the size range 1 to 3.3  $\mu\text{m}$ .

The tungsten metal is reduced from either tungsten trioxide ( $\text{WO}_3$ ), tungstic acid ( $\text{H}_2\text{WO}_4$ ), or ammonium paratungstate  $5(\text{NH}_4)_2\text{O} \cdot 12\text{WO}_3 \cdot x\text{H}_2\text{O}$ . In ammonium paratungstate, when  $x$  is 11, an orthorhombic unidecahydrate is formed which has a needle-shaped particle morphology and when  $x$  is 5, a monoclinic pentahydrate is formed which yields a cubic or equiaxed monoclinic morphology<sup>15, 16</sup>. These compounds are produced from the ores, wolframite  $(\text{Fe},\text{Mn})\text{WO}_4$  or scheelite  $(\text{CaWO}_4)$ <sup>5, 17-20</sup>. The production of solid ammonium paratungstate is an intermediate purification step in the extraction of tungsten from the above-mentioned ores<sup>21</sup>.

TABLE 1

APT PRODUCTION FLOW CHART



Economics favor starting with the ores only where the residual of the extraction processing can be used in steel making. The combination of steel and carbide productions permits a 95% recovery of the tungsten content from the ore. In addition, synthetic sheelite obtained from tungsten or tungsten carbide scrap can be processed along with naturally occurring sheelite<sup>22</sup>. These sheelites are converted into ammonium paratungstate. Table I demonstrates the steps involved in this purification process. On the same table, the process initiated with wolframite is also illustrated.

Reduction of ammonium paratungstate is generally accomplished in two steps. First, a thermal decomposition is performed to yield tungsten trioxide when heated in air and "blue oxide" ( $\text{WO}_{2.90}$ ) when heated in an inert atmosphere. In the second step, the resultant tungsten oxide is reduced in hydrogen to tungsten metal<sup>15</sup>.

The effect of process variables on the tungsten crystallite size during the reduction of tungsten oxide have been studied by numerous investigators<sup>5, 10, 23-28</sup>. A large variety of parameters have been identified as influencing the particle size. These experimenters have concluded that the grain size is dependent on (1) the starting material, (2) the reaction temperature, (3) the water content of the hydrogen, (4) the flow rate of the hydrogen, (5) the rate of passage of the reducing oxides through the furnace, and (6) the depth of the oxide bed. Particle sizes from 0.02 to 50  $\mu\text{m}$  were found in these studies. These studies have not addressed the direct reduction of ammonium paratungstate or discussed the mechanism of control of the particle size.

#### EXPERIMENTAL METHOD

The ammonium paratungstate (G.T.E. Sylvania, Towanda, PA) used in this study had a density of  $2.48 \text{ g cm}^{-3}$ . The material contained 25 ppm sodium and 10 ppm silicon.

The gases used in the experiments were High Purity helium 99.99% and 9.999% hydrogen (High Purity) with a dew point of  $-65^\circ\text{C}$  (Matheson Gas Products, Inc., East Rutherford, NJ).

X-Ray diffraction data was obtained using copper  $K_\alpha$  radiation with a nickel filter.

Scanning electron microscopy was performed with the sample coated with a sputtered layer of gold-palladium on the surface to avoid surface charging. Coating was unnecessary for the tungsten metal samples.

Thermogravimetric analysis was carried out in a 16 mm high alumina crucible using a Mettler Recording Vacuum Thermoanalyzer. The specific conditions for each analysis are shown with the data. Differential thermal gravimetry (DTG) was used to analyze the data. The alumina crucible was covered during one set of experiments. The cover was high alumina with a 1.3 mm hole in the center. Heating rates ranged from 2 to  $10^\circ\text{C min}^{-1}$ , sample sizes from 300 to 3000 mg and hydrogen flow rates over the sample from 10 to 30  $\text{l h}^{-1}$ .

The particle size measurements were made using two techniques. The first was by measurement of crystallite size from the micrographs. The second method

was X-ray diffraction line broadening. This method allowed the average size to be determined for samples with sizes less than 1000 Å. The (110) plane was used for comparison.

## RESULTS AND DISCUSSION

X-Ray diffraction analysis of the ammonium paratungstate (APT) indicated the presence of two phases. The major phase was ammonium pentahydrate  $5(\text{NH}_4)_2 \cdot 0.12\text{WO}_3 \cdot 5\text{H}_2\text{O}$ . The secondary phase was ammonium tungstate hydrate  $(\text{NH}_4)_2\text{WO}_4 \cdot n\text{H}_2\text{O}$ .

Thermogravimetric analysis (TGA) of the sample allowed identification of the sequence of decomposition and reduction reactions occurring during heat treatment. TGA in helium indicated a total weight loss of 10.31% with the reactions completed by 560°C. Through this temperature range there were four DTGA peaks typical of the decomposition of ADT to  $\text{WO}_{2.95}$ .

The sample was then run in hydrogen and the results can be seen in Fig. 1. The low temperature part of the reaction is unchanged from the results in helium, the APT decomposes to  $\text{WO}_{2.95}$ . Combining the TG data and X-ray diffraction data the reduction sequencey from  $\text{WO}_{2.95}$  to W metal was determined.

The first four peaks to 500°C represent dehydration of the APT. Through this region the X-ray peaks are decreasing in intensity (i.e. the ammonium pentahydrate and ammonium tungsten hydrate are decreasing in concentration). By 230°C, extensive cracking is evident in the APT powder. At 310°C, X-ray diffraction indicates only a broad roll at the  $d$ -spacing for the major peak of  $\text{WO}_{2.95}$ . This is typical of very small crystallites of this phase. By 410°C the  $\text{WO}_{2.95}$  phase can be easily identified. In each case the X-ray diffraction pattern clearly identified the phase present. The individual grains continue to fracture on heating and the metallic

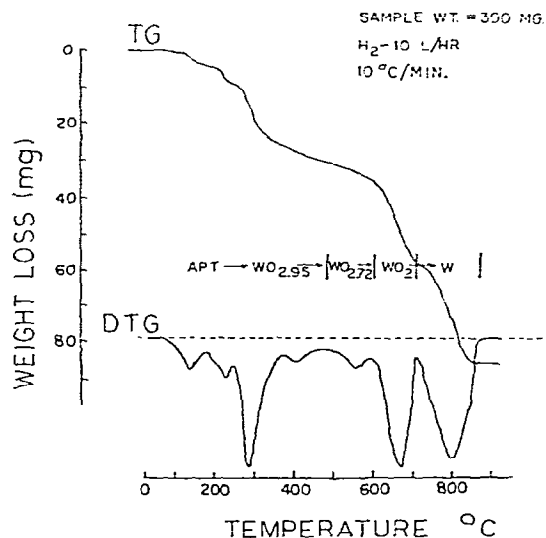


Fig. 1. Thermal analysis data for the reduction of APT in hydrogen.

tungsten particles seem to form on the surface by  $670^{\circ}\text{C}$ . The final product resembles the original APT only at low magnification. At higher magnifications it can be seen that there are small tungsten crystallites comprising the remanent structure of the APT. These crystallites are, of course, too small for use in bonded tungsten carbides.

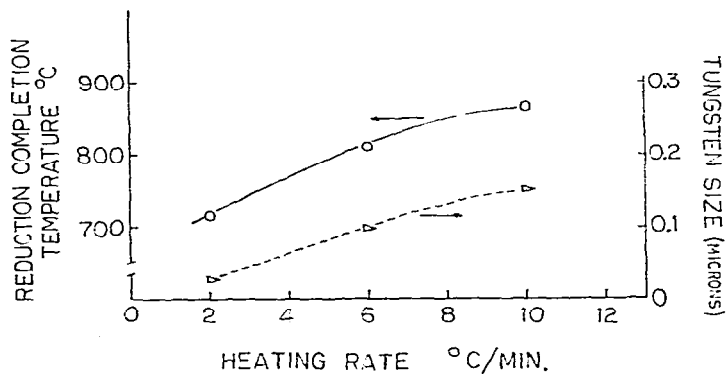


Fig. 2. The effect of heating rate on the tungsten crystallite size.

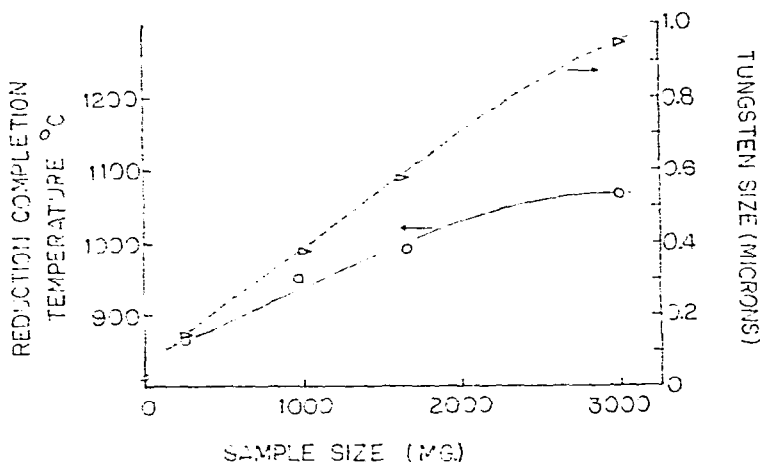


Fig. 3. The effect of sample size on tungsten crystallite size.

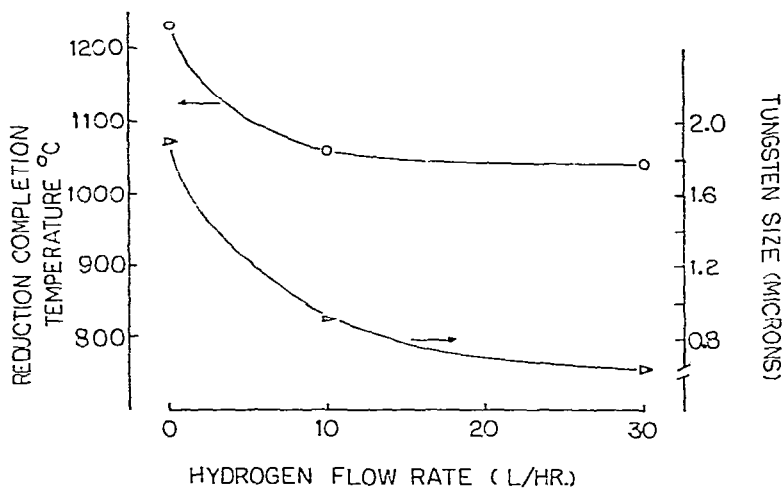


Fig. 4. The effect of hydrogen flow rate on the tungsten crystallite size.

In order to increase the crystallite size and understand the reaction mechanism studies were undertaken to determine the effect of (1) heating rate, (2) sample size, (3) hydrogen flow rate.

The effect of the rate of heating on the tungsten crystallite size was the first process variable studied. The samples were held isothermally at 950°C for 30 min and then cooled rapidly.

Figure 2 shows that the tungsten particle size increases from 0.026  $\mu\text{m}$  at 2°C  $\text{min}^{-1}$  to approximately 0.15  $\mu\text{m}$  at 10°C  $\text{min}^{-1}$ . The more rapid the heating rate, the larger the crystallite size. The completion temperature of the reduction reaction increases with increasing heating rate. It has been observed that an increase in the final reduction reaction completion temperature results in an increase in the tungsten crystallite size.

The effect of sample size was explored using 300, 975, 1650 and 3000 mg samples. These four sizes were heated at 10°C  $\text{min}^{-1}$ . Figure 3 shows that the crystallite size increases with increasing sample size. The tungsten reduction completion temperature increases as the sample size increases. The size of the tungsten crystals reaches almost 1  $\mu\text{m}$ .

The effect of hydrogen flow rate was also investigated as a process variable. A sample size of 300 mg was heated at 10°C  $\text{min}^{-1}$  to the reaction completion temperature with a hydrogen flow rate of 10 l  $\text{h}^{-1}$  and 30 l  $\text{h}^{-1}$ . As can be seen in Fig. 4 the higher hydrogen flow rate reduced the tungsten crystallite size. The higher hydrogen flow rate also decreases the tungsten reduction completion temperature.

The decrease in tungsten size is not large and suggests that the rate of 10 l  $\text{h}^{-1}$  is reasonably effective in sweeping the reaction products away from the reaction site. Consequently, this indicates that a stagnant hydrogen atmosphere would have a substantial effect in increasing the crystallite size. To test this hypothesis the alumina crucible holding the sample was capped. The cap had a small hole to allow the pressure to be maintained at one atmosphere. The atmosphere surrounding the capped crucible had a flow rate of 10 l  $\text{h}^{-1}$ .

The results of this experiment are also shown in Fig. 4 and are quite dramatic. The crystallite size increases from 1 to 1.9  $\mu\text{m}$ . The final reaction completion temperature rises to about 1230°C.

Increasing the sample size, reducing the hydrogen flow rate and increasing the heating rate all increased the size of the tungsten and increased the temperature at which the reduction reaction occurred as well as its final completion temperature. All of these steps had the effect of keeping the reaction products in the vicinity of the reaction site, or, put more positively, increasing the water/hydrogen ratio (i.e. the oxygen partial pressure) over the sample. With a constant hydrogen flow rate the more rapid heating rate provides less time to remove the reaction products. The larger sample size with a constant hydrogen flow rate has the effect of generating a larger quantity of reaction products. Capping of the crucible holds the reaction products at the site. These steps affect the solid-state reactions which require nucleation of the desired phase and subsequent crystal growth. The nucleation process occurs

at a lower temperature than the temperature of maximum crystal growth. The partial pressure of oxygen over the sample controls the rate of reduction of the  $WO_2$ . By retarding the reaction rate there is only limited opportunity for nuclei to form at low temperatures and consequently these nuclei grow to a larger size as the available tungsten oxide is reduced. Conversely, when the reaction proceeds rapidly at low temperatures, large numbers of nuclei form and the resultant crystal size is relatively small.

#### CONCLUSION

It has been shown that APT can be directly reduced to tungsten metal with a particle size suitable for practical use in cobalt bonded tungsten carbides. Control of the process variables is required to inhibit nucleation and restrict the number of sites at which reduction occurs.

#### ACKNOWLEDGEMENTS

The authors gratefully acknowledge: Professors M. G. McLaren, G. W. Phelps, J. R. Trout, Dr. J. B. Lambert, V. R. Wesson and Dr. Art Dana, V. R. Wesson, for reviewing this work; Dr. Ronald L. Peters for his cooperation and suggestions, Dr. B. K. Speronello for his technical assistance and V. R. Wesson for his support of this research program.

#### REFERENCES

- 1 A. Hara and M. Miyake, *Panseeber. Pulvermetall.*, 18 (1970) 2.
- 2 A. Hara and M. Miyake, *Nippon Kinzoku Gakkaishi*, 33 (1969) 12.
- 3 A. Hara and M. Miyake, *Monatsh. Chem.*, 103 (1972) 5.
- 4 A. Miyoshi and Y. Doi, *Funtai Oyobi Funmatsuyakin*, 11 (1964) 3.
- 5 P. Schwarzkoph and R. Kieffer, *Cemented Carbides*, MacMillan, New York, 1960.
- 6 M. Petrdlik and V. Dufek, *Hutm. Listy*, 10 (1955) 528.
- 7 L. D. Brownless, R. Edwards and T. Raine, *Iron Steel Inst. Rept. No. 58*, London, 1956.
- 8 J. Gurland, *J. Met.*, 6 (1954) 285.
- 9 G. S. Kreimer, O. S. Sanfonowa and J. Baranow, *Zh. Tekh. Fiz.*, 25 (1955) 117.
- 10 D. Duzevic and A. Milosevic, *Poroshk. Metall.*, 11 (1974) 102.
- 11 H. L. Patts, *Carbide J.*, 5 (1973) 6.
- 12 J. Gurland and P. Bardzil, *J. Met.*, 7 (1955) 311.
- 13 J. Gurland and J. T. Norton, *Second Plansee Seminar*, 1956.
- 14 N. Ingelstrom and H. Nordberg, *Eng. Fract. Mech.*, 6 (1974).
- 15 J. Gurland, *Society of Manufacturing Engineers Paper*, Dearborn, Michigan, 1971.
- 16 A. K. Basu and F. R. Sale, *J. Mater. Sci.*, 10 (1975).
- 17 B. E. Berry, *Murex Rev.*, 1 (1951) 165.
- 18 H. Alterthum, *Wolfram: Fortschritte in der Herstellung and Anwendungii, den hetzten Jahren*, Wolfram, Viewag und Sohn, Braunschweig, 1925.
- 19 F. Knepper, *Die Frabrikation von Wolframdrahten fur elektrische Gluhlampen und Radiorohren*, Hacimeister und Thal, Leipzig, 1930.
- 20 K. C. Li and C. Y. Wang, *Tungsten*, Reinhold, New York, 1947.
- 21 W. Ryan, *Non-ferrous Extractive Metallurgy in the United Kingdom*, Institution of Mining and Metallurgy, London, 1968.



- 22 *Powder Metallurgy*, Tech. Assistance Mission No. 141, Organization for European Economic Co-operation, Paris, 1955.
- 23 M. Kiyomiya, *Jpn. Pat.* 02,677, 1974.
- 24 M. Kiyomiya and I. Azeki, *Jpn. Pat.* 18,208, 1972.
- 25 O. K. Park and K. Y. Eun, *Kumsok Hakhoe Chi*, 11 (1973).
- 26 W. H. Bleeker, *Fr. Pat.* 2,088,431.
- 27 A. Talcashima, *Jpn. Pat.* 15,361, 1972.
- 28 G. A. Meerson and G. S. Kreimer, *Izv. Vyssh. Uchebn. Zaved Tsvetn. Metall.*, 15 (1972).